A liquid chromatography-mass spectrometry platform for the analysis of phyllobilins, the major degradation products of chlorophyll in Arabidopsis thaliana

Christ, Bastien ; Hauenstein, Mareike ; Hörtensteiner, Stefan

Abstract: During senescence, chlorophyll is broken down to a set of structurally similar, but distinct linear tetrapyrrolic compounds termed phyllobilins. Structure identification of phyllobilins from over a dozen plant species revealed that modifications at different peripheral positions may cause complex phyllobilin composition in a given species. For example, in Arabidopsis thaliana wild-type, eight different phyllobilins have structurally been characterized to date. Accurate phyllobilin identification and quantification, which classically have been performed by high performance liquid chromatography (HPLC) and UV/vis detection, are, however, hampered because of their similar physiochemical properties and vastly differing abundances in plant extracts. Here we established a rapid method for phyllobilin identification and quantification that couples ultra-HPLC with high-resolution/high-precision tandem mass spectrometry. Using Arabidopsis wild-type and mutant lines that are deficient in specific phyllobilin-modifying reactions, we identified a total of 16 phyllobilins, among them two that have not been described before in Arabidopsis. The single and collision-induced dissociation tandem mass spectrometry data of all 16 Arabidopsis phyllobilins were collected in a mass spectrometry library, which is available to the scientific community. The library allows rapid detection and quantification of phyllobilins within and across Arabidopsis genotypes and we demonstrate its potential use for high-throughput approaches and genome-wide association studies in chlorophyll breakdown. By extending the library with phyllobilin data from other plant species in the future, we aim providing a tool for chlorophyll metabolite analysis as a measure of senescence for practical applications, such as post-harvest quality control.

DOI: https://doi.org/10.1111/tpj.13253

Technical advance

A liquid chromatography-mass spectrometry platform for the analysis of phyllobilins, the major degradation products of chlorophyll in *Arabidopsis thaliana*

Bastien Christ[1,†], Mareike Hauenstein[†], Stefan Hörtensteiner*

Institute of Plant Biology, University of Zurich, Zollikerstrasse 107, CH-8008 Zurich, Switzerland

[†]These authors contributed equally to this manuscript

*For correspondence (email: shorten@botinst.uzh.ch)

[1]Current address: Whitehead Institute for Biomedical Research, 9 Cambridge Center, Cambridge, MA 02142-1479, USA

SUMMARY

During senescence, chlorophyll is broken down to a set of structurally similar, but distinct linear tetrapyrrolic compounds termed phyllobilins. Structure identification of phyllobilins from over a dozen plant species revealed that modifications at different peripheral positions may cause complex phyllobilin composition in a given species. For example, in *Arabidopsis thaliana* wild-type, eight different phyllobilins have structurally been characterized to date. Accurate phyllobilin identification and quantification, which classically have been performed by HPLC and UV/Vis detection, are, however, hampered because of their similar physiochemical properties and vastly differing abundancies in plant extracts. Here we established a rapid method for phyllobilin identification and quantification that couples ultra-high performance liquid chromatography with high-resolution/high-precision tandem mass spectrometry. Using Arabidopsis wild-type and mutant lines that are deficient in specific phyllobilin-modifying reactions, we identified a total of 16 phyllobilins, among them two that have not been described before in Arabidopsis. The single and collision-induced dissociation tandem mass spectrometry data of all 16 Arabidopsis phyllobilins were collected in a mass spectrometry library, which is available to the scientific community. The library allows rapid detection and quantification of phyllobilins within and across Arabidopsis genotypes and we demonstrate its potential use for high throughput approaches and genome-wide association studies in chlorophyll breakdown. By extending the library with phyllobilin data from other plant species in the future, we aim providing a tool for chlorophyll metabolite analysis as a measure of senescence for practical applications, such as post-harvest quality control.

SIGNIFICANCE STATEMENT

We established an LC-MS/MS platform that allows the simultaneous detection and quantification of several phyllobilins, i.e. the final products of chlorophyll degradation, within metabolite extracts of senescent *Arabidopsis thaliana* leaves. A freely available library currently containing the MS/MS spectral data of 16 Arabidopsis phyllobilins can be used for screening purposes of Arabidopsis senescence mutants and ecotypes and, because of its extendibility, will allow analysis of chlorophyll breakdown in other plant species in the future.

KEYWORDS

chlorophyll catabolites, phyllobilins, LC-MS, senescence, metabolite database

INTRODUCTION

Chlorophyll, the most abundant plant pigment, is a key factor for the absorption of sun-light and for its conversion to chemical energy during photosynthesis. During leaf senescence however, the light-absorbing properties of chlorophyll may turn into thread, because the decline of the photosynthetic capacity together with the dismantling of the photosynthetic apparatus at this stage would leave behind a highly photo-dynamic molecule that may cause the excess production of reactive oxygen species leading to photo-oxidative damage (Hörtensteiner 2004). Thus, the degradation of chlorophyll, which marks the most obvious visual symptom of leaf senescence, is a key metabolic process that aims at avoiding such photo-oxidative damage to the senescing tissues. In addition, it allows the efficient remobilization of leaf nutrients, in particular phosphorous and nitrogen, to sink tissues like developing seeds or storage organs (Hörtensteiner and Feller 2002). Besides leaf senescence, chlorophyll breakdown also occurs during the ripening of many climacteric and non-climacteric fruits, and as a response to challenge with different biotic and abiotic stresses (Amir-Shapira *et al.* 1987, Christ *et al.* 2014, Müller *et al.* 2007, Mur *et al.* 2010).

Although first reports on chlorophyll catabolic activities are just over a century old (Willstätter and Stoll 1913), the fate of chlorophyll during breakdown remained enigmatic for many decades. In 1991, the structure of a first degradation product of chlorophyll from barley with a linear tetrapyrrole backbone was determined by mass spectrometry (MS) and 1- and 2-dimensional NMR techniques (Kräutler *et al.* 1991). Since then, more than 40 (final) linear tetrapyrrolic degradation products of chlorophyll from over 15 angiosperm species, including the model plant *Arabidopsis thaliana* (Arabidopsis), have been described (Christ and Hörtensteiner 2014, Kräutler and Hörtensteiner 2013). Nowadays, they are named phyllobilins, resembling their close structural similarity to heme-derived bilins (Kräutler 2014). All, except one (Müller *et al.* 2006), derive from the oxygenolytic cleavage of the chlorin macrocycle of pheophorbide *a*, an Mg- and phytol-free intermediate of chlorophyll breakdown, to a *primary* fluorescent chlorophyll catabolite (*p*FCC) (Figure 1). This reaction is catalyzed by the successive action of two enzymes, PHEOPHORBIDE *a* OXYGENASE (PAO) that converts pheophorbide *a* to red chlorophyll catabolite (RCC), and RCC REDUCTASE (RCCR) that reduces RCC to *p*FCC (Rodoni *et al.* 1997, Wüthrich *et al.* 2000). Biochemical and genetic analyses revealed RCC to be metabolically channeled by PAO/RCCR and not to accumulate in vivo. RCCR exhibits an intriguing stereospecificity, which causes the formation of one of two C16 epimers of *p*FCC, i.e. *p*FCC (Mühlecker *et al.* 1997) or *epi-p*FCC (Mühlecker *et al.* 2000), depending on the source of RCCR (for atom numbering of chlorophyll catabolites, see *p*FCC in Figure 1). Thus, for example, Arabidopsis has a type-1 RCCR and produces *p*FCC while the tomato RCCR is type-2 and forms *epi-p*FCC (Pružinská *et al.* 2007).

Apart from being derived from either *p*FCC or *epi*-*p*FCC, two major subgroups of phyllobilins can be distinguished: (C1-) formyl-(C19-) oxobilins, also termed nonfluorescent chlorophyll catabolites (NCCs) that are the ultimate products of chlorin macrocycle cleavage by PAO, while additional subsequent oxidative C1 deformylation yields (C1,19-) dioxobilin-type catabolites, termed dioxobilin-type nonfluorescent chlorophyll catabolites (DNCCs) (Figure 1). While different plant species produce chlorophyll catabolites of only one of the two subgroups, others like, for example, Arabidopsis accumulate both DNCCs and NCCs simultaneously. C1-deformylation in Arabidopsis is catalyzed by the cytochrome P450 monooxygenase CYP89A9, whose activity accounts for more than 90% of the phyllobilins accumulating in this species during senescence (Christ *et al.* 2013). In most cases, phyllobilins accumulate inside the vacuole (Hinder *et al.* 1996, Matile *et al.* 1988) as nonfluorescent catabolites (DNCCs or NCCs) that are derived from respective fluorescent precursors (DFCCs or FCCs) by non-enzymatic isomerization caused by the acidic nature of the vacuolar sap (Oberhuber *et al.* 2003). Thus, fluorescent breakdown intermediates (derived from *p*FCC) are the products of several further modification reactions that are known to occur during chlorophyll breakdown and that ultimately give rise to the great variety of structurally distinct phyllobilins found in plants. Most of these modifications happen in the cytosol and occur at five different (peripheral) positions within *p*FCC. Except for a hydroxylation of the $C3^2$-ethyl side chain, which seems to be common to all species investigated to date, other modifications occur in a species-specific manner, resulting in a defined set of phyllobilins that occur within one species. These modifications include $O8^4$-demethylation, $C3^2$-OH group glucosylation and/or malonylation, C18-vinyl group dihydroxylation, C2 and C4 hydroxymethylation and esterification of the $C12^3$ moiety with different alcohols (Christ and Hörtensteiner 2014, Kräutler 2014, Süssenbacher *et al.* 2014). Depending on the number of modifying activities present in a given species, complex phyllobilin mixtures may occur. For example, eight (nonfluorescent) phyllobilins have been structurally characterized from senescent leaves of the Col-0 wild-type of Arabidopsis (Christ *et al.* 2013, Pružinská *et al.* 2005, Süssenbacher *et al.* 2015) (see Table 1). METHYLESTERASE16 (MES16) is known in this species to catalyze $O8^4$ demethylation (Christ *et al.* 2012). Additional activities that catalyze $C3^2$ hydroxylation and subsequent glucosylation, or C2 or C4 hydroxymethylation can be postulated, but their molecular nature is unknown to date (Figure 1).

In the past, phyllobilin analysis was mainly performed by classical high performance liquid chromatography (HPLC) and phyllobilin identification was often based on UV/Vis spectra that are typical for different classes of (fluorescent and nonfluorescent) phyllobilins (Christ and Hörtensteiner 2014, Kräutler 2014). Once manually identified, selected and isolated compounds were then structurally characterized by MS and/or NMR techniques. Efficient phyllobilin analysis was and still is limited by several technical difficulties related to UV/Vis-HPLC-based methods. Thus, separation and/or identification of individual phyllobilins by HPLC may be hampered by the accumulation during

senescence of different phyllobilins but also unrelated metabolites that have similar physicochemical properties and, therefore, may be co-extracted together with the phyllobilin of interest. In addition, some phyllobilins only occur in trace amounts thereby escaping their spectra-based detection. The increasing availability of liquid chromatography (LC)-MS-based instruments that combine ultra-high performance liquid chromatography with mildly-ionizing electrospray ionization (ESI) and sensitive and highly accurate mass spectrometers started to advance the analysis of chlorophyll breakdown significantly (Rios *et al.* 2014a, Rios *et al.* 2014b, Rios *et al.* 2015). Thus, the aim of this work was to develop an LC-MS platform that allows the rapid and reliable detection, automatic identification and quantification of phyllobilins within complex metabolite extracts. Using this technology, we have identified 16 Arabidopsis phyllobilins, two of which have not been described to date, and characterized their collision-induced dissociation (CID) tandem MS (MS/MS) fragmentation patterns. Besides uploading the experimental MS and MS/MS spectral data to METLIN, we provide a freely available 'Arabidopsis phyllobilin MS library' on our website. Although the library was produced with a Bruker-Daltonics Compact-MS, the information contained within it can easily be transferred to other LC-MS systems. We demonstrate the usability of our platform for the analysis of phyllobilin diversity within 18 Arabidopsis ecotypes and thus provide a suitable system, for example, for identification of unknown enzymes involved in phyllobilin modification in genome-wide association studies. We also show that the platform can be used for identifying 'Arabidopsis-like' chlorophyll catabolites in different plant species. The future plan is to extend the library by adding MS data of additional 'non-Arabidopsis' phyllobilins.

RESULTS

Tandem MS-based identification of known and novel phyllobilins in wild-type Arabidopsis

In wild-type Arabidopsis (Col-0), seven non-isomeric nonfluorescent phyllobilins have been identified to date (Table 1) (Pruzinska *et al.* 2005; Christ *et al.* 2013; Süssenbacher *et al.* 2015). Traditionally, these catabolites have obtained a name that is composed of their plant origin (e.g. *At*, for *Arabidopsis thaliana*), the type of catabolite (e.g. NCC or DNCC) and an index, which is based on peak order or relative retention under standard reversed-phase HPLC (Ginsburg and Matile 1993, Kräutler and Hörtensteiner 2013). Here, we introduce an alternative nomenclature, which indicates the type of catabolite (DNCC or NCC) followed by its monoisotopic molecular mass [M], but ignores the plant origin of the phyllobilins (see Table 1 and below). Extracts of green and senescent Col-0 leaves were compared using LC-ESI-MS in the positive ion-mode (Figure 2). Base peak chromatogram (BPC) and extracted ion chromatogram (EIC) analysis indicated the likely presence of pseudo-molecular ions

$[M+H]^+$ for all seven known non-isomeric Arabidopsis phyllobilins within senescent samples. The absence of these peaks from green tissues indicated phyllobilins to be specific to senescent leaves and to produce the most intense MS-ions using our experimental set-up. To confirm their identity, we performed data-dependent MS/MS experiments on individual precursor ions. As shown in Figure 3a for DNCC_618, the most abundant phyllobilin in Col-0 (see Figure S1 for the MS and MS/MS data of all phyllobilins identified in this work), MS/MS experiments resulted in the formation of characteristic major fragment ions known to occur under CID conditions using different MS instruments and a wide range of collision energies (Müller *et al.* 2014, Rios *et al.* 2014a, Vergeiner *et al.* 2015) (see Table S1, for a structured list of the most abundant MS/MS fragments of each phyllobilin). Among them were fragments corresponding to the loss of pyrrole ring D and/or A. Interestingly, this analysis uncovered fragmentation pattern differences (Table S1) for two almost equally abundant isomers of DNCC_632, termed DNCC_632-1 and DNCC_632-2 that differ at the site of hydroxymethylation (Figure S1; Table 1; see Figure S2, for respective EICs). As shown earlier (Süssenbacher *et al.* 2015), hydoxymethylation at C2 (as in DNCC_632-2) favored loss of this group in MS/MS mode, as compared to the C4-hydroxymethylated isomer (i.e. DNCC_632-1) (Table S1).

$O8^4$-demethylated phyllobilins readily loose the $C8^2$ carboxyl group in MS/MS experiments, while loss of MeOH is typically found in phyllobilins containing an intact $C8^2$ carboxymethyl ester (Müller *et al.* 2014). Accordingly, a fragment ion with m/z 337.12 that corresponded to $[M+H\text{-(rings D+A)-}H_2O]^+$ for $O8^4$-demethylated phyllobilins and to $[M+H\text{-(rings D+A)-}CH_3OH]^+$ for phyllobilins with an intact $C8^2$ carboxymethyl ester, commonly and abundantly occurred in MS/MS experiments (Table S1). Similarly, $C8^2$-demethylated Arabidopsis phyllobilins exhibited a common prominent neutral loss of 167.06 mass units $[M+H\text{-(ring D+}CO_2)$ in MS/MS mode. Using these characteristic features an additional phyllobilin was identified in senescent wild-type samples. The analysis of its MS/MS fragmentation pattern (Figure 3b; Figure S1; Table S1) allowed attribution to a novel DNCC, i.e. DNCC_780, the glucosylated derivative of DNCC_618.

In the course of our analysis, we detected another, low abundant DNCC, DNCC_648 (Figure S3a) in which most MS/MS fragments were shifted by 30 mass units compared to DNCC_618 indicating DNCC_648 to be potentially hydroxymethylated. However, when performing extractions of senescent Col-0 leaves using deuterated methanol, the mass of DNCC_648 was shifted by three mass units (Figure S3b), indicating this metabolite to be an extraction artifact derived from methoxylation of DNCC_618, the most abundant phyllobilin in Col-0 extracts. Similarly, an additional low abundant NCC, NCC_646, seemed to be the oxidation product of NCC_630. Such oxidation/methoxylation products of phyllobilins have been described before and their occurrence was attributed to enzymatic activities present in leaf extracts of *Spathipyllum wallisii* (Vergeiner *et al.* 2015). Such activities are obviously also present in Arabidopsis. As shown in Figure S3c for two methoxylated derivatives of phyllobilins

found in the *cyp89a9-1* mutant (see below), the formation of oxidated/methoxylated phyllobilins can be minimized by rapid extraction and work-up of senescent leaves under cold working conditions as described in Experimental Procedures.

Absence of *p*FCC-modifying enzymes affects phyllobilin composition

Of several *p*FCC-modifying activities that ultimately lead to the diverse set of phyllobilins found in Arabidopsis, so far only CYP89A9 and MES16 have been identified at the molecular level (Christ *et al.* 2012, Christ *et al.* 2013). We analyzed respective mutants, i.e. *cyp89a9-1*, *mes16-1* and a *cyp89a9-1*/*mes16-1* double mutant. Figure 4 compares BPCs and EICs of senescent leaves of the three mutant lines. As expected, *cyp89a9-1* did not produce dioxobilin-type catabolites (Table 1), but instead accumulated high amounts of respective NCCs (Christ *et al.* 2013) and all phyllobilins identified in *mes16-1* possessed an intact $C8^2$-carboxymethyl ester.

As described above for Col-0, extraction of MS/MS-based characteristic NLCs and EICs and subsequent full MS/MS analysis allowed the identification of one novel phyllobilin in *mes16-1*, DNCC_794 that corresponds to the respective demethylated wild-type catabolites, i.e. DNCC_780 (Tables 1 and S1; Figure S1). Further likely phyllobilins were, similar to DNCC_648 in Col-0, artifactual oxidation/methoxylation products of the most abundant phyllobilins occurring in respective mutants that were produced during extraction. Since under optimal extraction conditions (Figure S3c) these occurred only in trace amounts, they were not further considered.

Absence of MES16 has been shown to impact the non-enzymatic isomerization of (D)FCCs to (D)NCCs, causing the accumulation of relatively high amounts of fluorescent catabolites during senescence (Christ *et al.* 2012). As several of the phyllobilins detected here occurred as isomers with different LC retention times (Figure S2), it seemed possible that these represented respective (D)FCC isomers. However, this was not restricted to MES16-deficient lines. In addition, under the acidic extraction and LC-MS conditions used here (see Experimental Procedures) fluorescent catabolites were most likely rapidly converted to their (isomeric) nonfluorescent products. In line with this, as an example, the retention time of the most abundant isomer of NCC_806, a phyllobilin present in all four investigated lines (Table 1), was unaltered in all lines (Figures 2 and 4; see Figure S2, for respective EICs), while under standard (neutral) HPLC conditions, fluorescent catabolites have shifted retention times as compared to their nonfluorescent counterparts (Christ *et al.* 2012). Thus, the nature of phyllobilin isomers, several of which have already been described in the literature (Süssenbacher *et al.* 2014, Süssenbacher *et al.* 2015) remains unsure. For quantification (see below), they were treated as 'one' phyllobilin.

Phyllobilin identification and quantification by an 'Arabidopsis phyllobilin MS library'

Using classical HPLC and UV/Vis-based peak integration as a measure of quantity, we have shown earlier that the total abundance of phyllobilins that accumulate in senescent Arabidopsis wild-type and *cyp89a9-1* leaves accounts for almost all the degraded chlorophyll in these lines (Christ *et al.* 2013). Since neither standards are available for any of the Arabidopsis phyllobilins that would allow for their exact quantification in MS experiments, nor the relative efficiency of MS ionization of different types of phyllobilins is known, we reasoned to compare UV/Vis- with ion intensity-based quantities of phyllobilins in different mutant backgrounds that are not compromised in chlorophyll breakdown *per se*.

Firstly, high-resolution/high-precision MS and MS/MS data for the 16 Arabidopsis phyllobilins described above were compiled into a mass spectral library using LibraryEditor and DataAnalysis (Bruker Daltonics, Bremen, Germany). Subsequently, LC–MS data acquired in data-dependent MS/MS mode from wild-type, *mes16-1* and *cyp89a9-1* were processed using the 'Find Molecular Features' (FMF) peak detection algorithm of DataAnalysis (Bruker Daltonics), which combines isotopes, charge states, adducts and neutral losses belonging to the same compound into one feature. FMF compounds corresponding to phyllobilins were automatically identified using the Arabidopsis phyllobilin MS library and were quantified using the relative abundance value provided by the FMF algorithm (further details are available in the Experimental Procedures). Finally, UV/Vis peaks were quantified at 254 nm (Figure 2), the wavelength most suitable for determining DNCC and NCC abundancies (Christ *et al.* 2013). Despite significant variation in phyllobilin composition, causing distinct clustering of the genotypes in a principle component analysis performed on the entire LC-MS spectra data (Figure 5a), the three lines were expected to accumulate similar phyllobilin quantities. Indeed, overall absorption-based relative quantities matched MS-ion intensities for each analyzed genotype (Figure 5b), demonstrating that MS ionization efficiency is independent of the type of phyllobilin (e.g. DNCCs vs NCCs, methylated vs demethylated phyllobilins). This rendered potential matrix effects rather unlikely and, thus, allowed absolute quantification with high confidence using one external phyllobilin standard. Accordingly, we used *Cj*-NCC-1 (m/z 645.292; $[M+H]^+$), a well-studied phyllobilin from *Cercidiphyllum japonicum* (Müller *et al.* 2014) that is a C16 stereoisomer of NCC_644 of Arabidopsis, as standard. To further confirm the usability of *Cj*-NCC-1 as an external rather than internal standard, we compared ion intensities of the standard within the used concentration range in the absence and presence of senescent leaf extracts from Col-0 (that does not form NCC_644). Figure S4a shows that ion intensity of the standard is unchanged upon addition of Arabidopsis plant extracts, indicating that ion suppression does not occur and calibration obtained using *Cj*-NCC-1 as the external standard can be used for phyllobilin quantification from plant extracts. Finally, matrix effects potentially deriving from the LC system were analyzed by comparing phyllobilin ion intensity from identical Col-0 samples using different LC elution

conditions. Figure S4b shows that changes in the LC program had no effect on the quantity of individual phyllobilins or their total abundance.

We used the *Cj*-NCC-1 standard to determine absolute phyllobilin quantities in the different mutant lines (Figure 5c) and to correlate their abundance to the amount of degraded chlorophyll (Figure 5d). This analysis showed that in all investigated lines, the abundance of phyllobilins accumulating during senescence corresponds to about 60-70% of degraded chlorophyll. The fate of the missing fraction remains unclear to date, but possibly further, so far unidentified, phyllobilins are formed, or a certain fraction of the phyllobilins is further degraded.

Applications for the open-source Arabidopsis phyllobilin MS library

The Arabidopsis phyllobilin MS library that contains the spectral data analyzed here and the DataAnalysis method are available from our webpage (http://www.botinst.uzh.ch/research/physiology/horten/ms-library.html) and can be used to analyze samples for the presence of phyllobilins on Bruker platforms. In addition, the MS and MS/MS data of each individual phyllobilin are deposited on our webpage in the widely used mzXML (m/z extensible markup language) format that allows their incorporation into MS data analysis platforms from many suppliers. MS data of all phyllobilins described here were also uploaded on METLIN (https://metlin.scripps.edu/index.php) (Smith *et al.* 2005).

The usefulness and robustness of the Arabidopsis phyllobilin MS library in detecting and quantifying phyllobilins across a large number of senescent leaf samples was tested by identifying and determining relative phyllobilin abundance in a set of 18 *Arabidopsis thaliana* wild-type accessions (Figure 6a-d). Interestingly, this experiment reveals that the proportion of phyllobilins that are hydroxylated does not dramatically vary among Arabidopsis ecotypes whereas deformylated, demethylated and $O3^2$-glucosylated phyllobilins accumulate in different amounts. We further investigated the library's capacity in identifying phyllobilins in plant species, such as *Brassica napus* (canola), *Spinacia oleracea* (spinach) and *Pyrus communis* (pear) that are known to contain one or more 'Arabidopsis-like' phyllobilins (Berghold *et al.* 2002, Mühlecker and Kräutler 1996, Müller *et al.* 2007, Oberhuber *et al.* 2001) (Figure 6e). Most of the expected phyllobilins could indeed be identified. As spinach and pear possess a type-2 RCCR, while the one of canola and Arabidopsis is type-1 (Hörtensteiner *et al.* 2000, Kräutler 2014), the phyllobilins detected in spinach and pear are C16-epimers of respective Arabidopsis phyllobilins and were thus slightly shifted towards later retention times. Remarkably, use of the phyllobilin MS library enabled the identification of additional, so far undescribed, phyllobilins in canola and spinach. Among the novel canola phyllobilins were two rather low abundant DNCCs, indicating the presence in this species of a CYP89A9-like enzyme, whose activity may however be low in comparison to the Arabidopsis enzyme (Christ *et al.* 2013).

DISCUSSION

Chlorophyll breakdown is the most obvious sign of leaf senescence, but is also relevant during fruit ripening, seed maturation and desiccation in resurrection plants (Christ *et al.* 2014, Guyer *et al.* 2014, Moser *et al.* 2008a, Müller *et al.* 2007, Nakajima *et al.* 2012). In all plant species investigated so far, chlorophyll breakdown yields structurally similar linear tetrapyrroles, now termed phyllobilins (Kräutler 2014). These are ultimately derived from PAO that cleaves the chlorin macrocycle of the intermediate pheophorbide *a* (Hörtensteiner *et al.* 1998, Pružinská *et al.* 2003). Hence, the pathway of chlorophyll breakdown is now called the 'PAO/phyllobilin' pathway (Kräutler and Hörtensteiner 2013). Most of the naturally occurring phyllobilins are nonfluorescent forms of (C1-) formyl-(C19-) oxobilins (NCCs) or (C1,19-) dioxobilins (DNCCs) that are derived from respective isomeric fluorescent precursors (FCCs or DFCCs) through acid-catalyzed nonenzymatic isomerization inside the vacuole, their place of storage within senescing cells (Oberhuber *et al.* 2003). Exceptions are persistent so-called hypermodified FCCs identified in *Musa acuminata* and *S. wallisii* that are conjugated at $C12^3$, i.e. modifications that abolish their isomerization to NCCs (Banala *et al.* 2010, Kräutler *et al.* 2010, Moser *et al.* 2009). Isomerization was also shown to be slower in $O8^4$-methylated phyllobilins compared to respective demethylated ones, causing rather high accumulation of fluorescent phyllobilins in Arabidopsis *mes16-1* mutants that are deficient in the $O8^4$-methylesterase (Christ *et al.* 2012). Nevertheless, the data presented here for Arabidopsis (which does not form hypermodified catabolites) indicate that under the acidic extraction and LC-MS conditions used, fluorescent phyllobilins were (even in MES16-deficient lines) rather rapidly converted to respective nonfluorescent isomers.

Besides their possible occurrence as either fluorescent or nonfluorescent isomers, phyllobilins are divergent because of distinct side group modifications that occur in a species-specific manner. Thus, for example, in Arabidopsis, potential modifications at four positions (C2, $C3^2$, C4 and/or $O8^4$) have been described (Christ *et al.* 2012, Christ *et al.* 2013, Süssenbacher *et al.* 2014, Süssenbacher *et al.* 2015). Hydroxymethylation at C2 or C4 was considered to be linked to C1 deformylation by CYP89A9 and, thus, to only occur in DNCCs, while $C3^2$ hydroxylation (potentially followed by glucosylation) and hydroxymethylation were considered to exclude each other (Süssenbacher *et al.* 2015). Thus, ten DNCCs and six NCCs with distinct molecular constitution were expected to be present in senescent Arabidopsis leaves. The LC-MS platform presented here is able to identify all these 16 phyllobilins, whereby compounds with identical molecular composition (three DNCC_632 and two DNCC_646 isomers) can be distinguished by their MS/MS fragmentation patterns. For the two novel glucosylated DNCCs detected here, DNCC_780 and DNCC_794, tentative structures were assigned in analogy to

respective known glucosylated NCCs, NCC_792 and NCC_806; however, NMR studies that were beyond the scope of this work are required in the future to confirm their constitution. Several phyllobilins that occurred in trace amounts were shown to be oxidation/methoxylation products of respective abundant phyllobilins. As shown previously (Vergeiner *et al.* 2015) their formation can be minimized by rapid work-up of extracts under cold temperatures.

The Arabidopsis phyllobilin MS library presented in this work is based on the MS and MS/MS data of 16 identified phyllobilins of Arabidopsis. We demonstrate that the library can be used for phyllobilin detection and quantification during leaf senescence, to determine relative abundances of individual or groups of phyllobilins within and across Arabidopsis genotypes. In addition, the library was successful in identifying known and novel 'Arabidopsis-like' phyllobilins in other plant species. This included spinach and pear, which, because of the distinct stereospecificty of their RCCRs (Kräutler 2014, Oberhuber *et al.* 2001), produce the C16 epimers of the respective Arabidopsis phyllobilins.

State-of-the-art quantification in MS studies typically uses isotope labelled standards for each compound to be analyzed. Nevertheless, we choose to quantify phyllobilin abundance using one singly external standard. We rationalize this strategy as follows: (1) phyllobilins are not commercially available, (2) isolation of pure compounds is tedious and at best possible for the most abundant phyllobilins, but impossible for all, (3) isotope labelling would require an in vivo approach, likely causing ununiformed labeling, and (4) phyllobilins are not particularly stable in solution over long periods of time, which would require their regular isolation. Our evaluation of quantification using different mutants that produce different compositions of phyllobilins (Figure 5) and spiking the external standard with plant extracts (Figure S4) demonstrates the reliability of the chosen quantification method.

The LC-MS platform described here that combines ultra-high performance liquid chromatography with sensitive high-resolution/high-precision mass spectrometry has several advantages over traditional HPLC that has widely been used in the past to analyze chlorophyll breakdown in plants. Thus, it allows fast and sensitive phyllobilin identification with high resolution from complex plant extracts using a combination of different MS features such as NLC, EIC and MS/MS spectra. Thus, peak identification and quantification is independent from sole detection by UV/Vis absorption used in the past, which is often hampered by interference of unrelated compounds, in particular in senescent sample extracts. Finally, highly sensitive mass spectrometry enables the identification of even minor phyllobilins (for example DNCC_780) that have been overlooked in conventional HPLC. Together with the MS library established here, phyllobilin abundance can rather rapidly be quantified across many samples and replicates, allowing high throughput analysis in the future, e.g. for mutant screening purposes or genome-wide association studies.

Recently, a systematic LC-MS methodology was proposed that allows the detection of phyllobilins from sources not studied before (Rios *et al.* 2015). The approach applies EIC-based screening of plant samples against an MS library (created ex professo) that contains the pseudo-molecular masses of the 20 (non-isomeric) phyllobilins described in the literature to date. Compounds that match a certain threshold of mass precision and isotope patterning are subsequently analyzed by ion-trap fragmentation. If fulfilling criteria of fragmentation patterning that are scored based on published data or theoretical fragmentation prediction, identity of phyllobilins is finally confirmed by ESI-MS/MS. The approach and the tools provided here are distinct from the published methodology of Rios (Rios *et al.* 2015) because our library contains experimental MS as well as MS/MS data, which allows detection of phyllobilins in a given plant sample in a single LC-MS/MS run. Furthermore, structural isomers, like DNCC_632-1 and DNCC_632-2, can be distinguished with our method by their very distinct fragmentation patterns. Finally, employing "molecular feature" extraction algorithms (provided in MS data analysis programs of many suppliers) rather than EICs to screen plant samples for the presence of phyllobilins allows rapid and reliable compound quantification, as demonstrated here. A current limitation of our strategy is the fact that not all phyllobilins identified so far in different plant species are present in the library; however the Arabidopsis phyllobilin MS library and associated MS/MS data for individual phyllobilins that are accessible from our webpage (http://www.botinst.uzh.ch/research/physiology/horten/ms-library.html) will regularly be updated with newly identified phyllobilins in the future. This strategy plans to include phyllobilin data from crop plants, such as maize and barley (Berghold *et al.* 2006, Kräutler *et al.* 1991, Losey and Engel 2001), allowing future analysis of chlorophyll metabolites as a measure of senescence to be used for practical applications, as, for example, post-harvest quality control or senescence screening purposes in field trials.

Phyllobilins are abundant molecules in senescent leaf and fruit peel extracts, and likely also accumulate to rather high abundance under certain chlorophyll degradation-inducing stress conditions. Despite, to the best of our knowledge phyllobilin MS/MS data are not available in publicly accessible MS databases such as METLIN (Smith *et al.* 2005) or ReSpect (Sawada *et al.* 2012). Our work provides a first set of such data in METLIN and aims to promote the systematic addition of MS data of newly identified phyllobilins to public MS databases in the future.

EXPERIMENTAL PROCEDURES

Plant material

Arabidopsis thaliana ecotype Col-0 was used as the wild-type. Two T-DNA insertion lines were used in addition: *mes16-1* (SALK_139756; At4g16690) (Christ *et al.*, 2012) and *cyp89a9-1* (SM_3_39636; At3g03470) (Christ *et al.* 2013). The 18 Arabidopsis ecotypes used for the experiment shown in Figure 6 were from the Nordborg collection (Nordborg *et al.* 2005). All Arabidopsis lines were obtained from the European Arabidopsis Stock Center. Canola (*Brassica napus* cv. Bonanza) was obtained from a local seed company.

Plants were grown on soil in 12-h-light/12-h-dark photoperiod under fluorescent light of 80 to 120 µmol photons m^{-2} s^{-1} at 22°C and 60% relative humidity. For senescence induction, leaves from 5-week-old Arabidopsis or 2-week-old canola plants were excised and incubated in permanent darkness on wet filter paper at ambient temperature until they turned yellow (between 8 d and 16 d depending on the ecotype).

Pear fruits (*Pyrus communis* cv. Conference) and spinach leaves (*Spinacia oleracea*) were obtained from a local food store.

Phyllobilin extraction

Leaves were collected in 2-mL Eppendorf tubes containing 400-500 µl of 1.25-1.65 mm glass beads, weighted and immediately frozen in liquid nitrogen. The frozen samples were ground using a MM300 Mixer Mill (Retsch, Germany) at 30 Hz for 5 min and stored at -80°C until further processing. Phyllobilins were extracted using 5 volumes (w/v) of extraction buffer (80% methanol, 20% water, 0.1% formic acid [v/v/v] and 1 µg mL^{-1} ampicillin as internal standard) precooled to –20°C. Extracts were homogenized at 30 Hz for 5 min in the cold and centrifuged (16'000g, 4°C). After re-centrifugation, supernatants were transferred to LC vials, randomized and analyzed by LC-MS. Note that rapid extraction and work-up under cold conditions is essential to prevent artifactual oxidation/methoxylation reactions to occur (Vergeiner *et al.* 2015).

Quantification of chlorophyll

Samples were collected and extracted as described for phyllobilins with the following modifications: chlorophyll was extracted in 10% (v/v) 0.2 M Tris-HCl, pH 8.0, in acetone, precooled to –20°C (5 mL g^{-1} fresh weight). After centrifugation twice (4 min, 16'000g, 4°C), supernatants were analyzed spectrophotometrically (Strain *et al.* 1971).

LC-MS/MS analysis

The LC-MS/MS instrument was composed of a Thermo Scientific Dionex Ultimate 3000 Rapid Separation LC system (Thermo Fisher Scientific, Reinach, Switzerland) equipped with a photodiode array detector coupled to a Bruker Compact ESI-Q-TOF (Bruker Daltonics). The reverse-phase system

consisted of an ACQUITY UPLC™ BEH C18 column (1.7 µm, 2.1 x 150 mm; Waters, Milford, MA, USA) which was developed using LC-MS/MS-grade solvents (Chemie Brunschwig, Basel, Switzerland) with a gradient (flow rate of 0.3 mL min^{-1}) of solvent B (acetonitrile with 0.1% [v/v] formic acid) in solvent A (water with 0.1% [v/v] formic acid) as follows (all v/v): 30% for 0.5 min, 30% to 70% in 7.5 min, 70% to 100% in 0.1 min and 100% for 3.9 min. ESI source conditions were set as follows: gas temperature, 220°C; drying gas, 9 L/min; nebulizer, 2.2 bar; capillary voltage, 4500 V; end plate offset, 500 V. Tuning conditions were set as follows: funnel 1 RF, 250 Vpp; funnel 2 RF, 150 Vpp; isCID energy, 0 eV; hexapole RF, 50 Vpp; quadrupole ion energy, 3.0 eV; quadrupole low mass, 90 m/z; collision cell, 6 eV; pre-pulse storage time, 3 µs. The instrument was set to acquire over the m/z range 50 - 1300, with an acquisition rate of 4 spectra s^{-1}. Conditions for MS/MS of automatically selected precursors (data-dependent MS/MS) were set as follows: threshold, 1000 counts; active smart exclusion (5x); active exclusion (exclude after 3 spectra, release after 0.2 min, reconsider precursor if current intensity/previous intensity is ≥5); number of precursors, 3; active stepping [basic mode, timing 50%-50%, collision RF from 350 to 450 Vpp, transfer time from 65 to 80 µs, collision energy ramped from 80 to 120% (see Table 1, for collision energies applied for each phyllobilin)]. All data were recalibrated internally using pre-run injection of sodium formate (10 mM sodium hydroxide in 0.2% formic acid, 49.8% water, 50% isopropanol [v/v/v]). Each sample was run in MS and data-dependent MS/MS modes. For absolute quantification of phyllobilins, purified *Cj*-NCC-1 obtained from B. Kräutler, University of Innsbruck, Austria, was used as standard (Moser *et al.* 2008b).

Data analysis

MS data were extracted and analyzed using DataAnalysis (version 4.2, Bruker Daltonics). A phyllobilin MS spectral library was built using LibraryEditor (version 4.2, Bruker Daltonics) by compiling MS and MS/MS spectra from known and newly identified phyllobilins. This library was further used in DataAnalysis to identify and quantify phyllobilins from samples analyzed in data-dependent MS/MS mode using the following DataAnalysis script: Analysis.RecalibrateAutomatically, Analysis.FindMolecularFeatures, Analysis.Compounds.Identify, Analysis.Compounds.ApplyFilter, Analysis.Save, Form.close. This script allows to automatically recalibrate, group MS and MS/MS spectra into molecular features (FMF algorithm), identify and quantify phyllobilins from multiple samples. Parameters for identification of molecular features and library identification are part of the DataAnalysis method file that is available on our website (http://www.botinst.uzh.ch/research/physiology/horten/ms-library.html). The compound table containing the relative amount of the molecular features identified as phyllobilins was copied into Excel (Microsoft Corporation, Redmond, WA, USA) for downstream calculation. For quantification of

phyllobilins using UV/Vis data, peak areas at 254 nm were determined in DataAnalysis and copied into Excel.

The PCA plot comparing Col-0, *mes16-1*, *cyp89a9-1* and *cyp89a9-1*/*mes16-1* (Figure 5a) was generated using XCMS online (Tautenhahn *et al.* 2012) as follows: MS data from samples analyzed in MS mode were converted to mzXML format using the program MSConvert (http://proteowizard.sourceforge.net/pubs.shtml) and uploaded to the XCMS online server (https://xcmsonline.scripps.edu/). A multigroup comparison of the three datasets was performed using the pre-set parameters 'UPLC / Bruker Q-TOF'.

ACKNOWLEDGEMENTS

We kindly thank Bernhard Kräutler, University of Innsbruck, Austria for providing *Cj*-NCC-1. Thanks to Marco Soldenhoff for design of the webpage containing the phyllobilin MS data. This work was supported by grants of the Swiss National Science Foundation (Nos. 31003A_149389/1 and 31CP30_163504/1) to S.H. The authors declare no conflicts of interest.

SUPPORTING INFORMATION

Additional Information may be found in the online version of this article.

Figure S1. MS and MS/MS spectra of all phyllobilins identified in this work.

Figure S2. Extracted ion chromatograms of all phyllobilins identified in Col-0 and different chlorophyll catabolic mutants.

Figure S3. Artifactual formation of methoxylated phyllobilins in Arabidopsis leaf extracts.

Figure S4. Analysis of ion suppression and matrix effects for phyllobilin quantification.

Table S1. MS/MS fragment ions of all phyllobilins identified in this work.

REFERENCES

Amir-Shapira, D., Goldschmidt, E.E. and Altman, A. (1987) Chlorophyll catabolism in senescing plant tissues: *In vivo* breakdown intermediates suggest different degradative pathways for *Citrus* fruit and parsley leaves. *Proc. Natl. Acad. Sci. USA*, **84**, 1901-1905.

Banala, S., Moser, S., Müller, T., Kreutz, C.R., Holzinger, A., Lütz, C. and Kräutler, B. (2010) Hypermodified fluorescent chlorophyll catabolites: source of blue luminescence in senescent leaves. *Angew. Chem. Int. Ed.*, **49**, 5174-5177.

Berghold, J., Breuker, K., Oberhuber, M., Hörtensteiner, S. and Kräutler, B. (2002) Chlorophyll breakdown in spinach: on the structure of five nonfluorescent chlorophyll catabolites. *Photosynth. Res.*, **74**, 109-119.

Berghold, J., Müller, T., Ulrich, M., Hörtensteiner, S. and Kräutler, B. (2006) Chlorophyll breakdown in maize: on the structure of two nonfluorescent chlorophyll catabolites. *Monatsh. Chem.*, **137**, 751-763.

Christ, B., Egert, A., Süssenbacher, I., Kräutler, B., Bartels, D., Peters, S. and Hörtensteiner, S. (2014) Water deficit induces chlorophyll degradation via the 'PAO/phyllobilin' pathway in leaves of homoio- (*Craterostigma pumilum*) and poikilochlorophyllous (*Xerophyta viscosa*) resurrection plants. *Plant Cell Environ.*, **37**, 2521-2531.

Christ, B. and Hörtensteiner, S. (2014) Mechanism and significance of chlorophyll breakdown. *J. Plant Growth Regul.*, **33**, 4-20.

Christ, B., Schelbert, S., Aubry, S., Süssenbacher, I., Müller, T., Kräutler, B. and Hörtensteiner, S. (2012) MES16, a member of the methylesterase protein family, specifically demethylates fluorescent chlorophyll catabolites during chlorophyll breakdown in Arabidopsis. *Plant Physiol.*, **158**, 628-641.

Christ, B., Süssenbacher, I., Moser, S., Bichsel, N., Egert, A., Müller, T., Kräutler, B. and Hörtensteiner, S. (2013) Cytochrome P450 CYP89A9 is involved in the formation of major chlorophyll catabolites during leaf senescence in *Arabidopsis*. *Plant Cell*, **25**, 1868-1880.

Ginsburg, S. and Matile, P. (1993) Identification of catabolites of chlorophyll porphyrin in senescent rape cotyledons. *Plant Physiol.*, **102**, 521-527.

Guyer, L., Schelbert Hofstetter, S., Christ, B., Silverstre Lira, B., Rossi, M. and Hörtensteiner, S. (2014) Different mechanisms are responsible for chlorophyll dephytylation during fruit ripening and leaf senescence in tomato. *Plant Physiol.*, **166**, 44-56.

Hinder, B., Schellenberg, M., Rodoni, S., Ginsburg, S., Vogt, E., Martinoia, E., Matile, P. and Hörtensteiner, S. (1996) How plants dispose of chlorophyll catabolites. Directly energized uptake of tetrapyrrolic breakdown products into isolated vacuoles. *J. Biol. Chem.*, **271**, 27233-27236.

Hörtensteiner, S. (2004) The loss of green color during chlorophyll degradation - a prerequisite to prevent cell death? *Planta*, **219**, 191-194.

Hörtensteiner, S. and Feller, U. (2002) Nitrogen metabolism and remobilization during senescence. *J. Exp. Bot.*, **53**, 927-937.

Hörtensteiner, S., Rodoni, S., Schellenberg, M., Vicentini, F., Nandi, O.I., Qiu, Y.-L. and Matile, P. (2000) Evolution of chlorophyll degradation: the significance of RCC reductase. *Plant Biol.*, **2**, 63-67.

Hörtensteiner, S., Wüthrich, K.L., Matile, P., Ongania, K.-H. and Kräutler, B. (1998) The key step in chlorophyll breakdown in higher plants. Cleavage of pheophorbide *a* macrocycle by a monooxygenase. *J. Biol. Chem.*, **273**, 15335-15339.

Kräutler, B. (2014) Phyllobilins - the abundant bilin-type tetrapyrrolic catabolites of the green plant pigment chlorophyll. *Chem. Soc. Rev.*, **43**, 6227-6238.

Kräutler, B., Banala, S., Moser, S., Vergeiner, C., Müller, T., Lütz, C. and Holzinger, A. (2010) A novel blue fluorescent chlorophyll catabolite accumulates in senescent leaves of the peace lily and indicates a divergent path of chlorophyll breakdown. *FEBS Lett.*, **584**, 4215-4221.

Kräutler, B. and Hörtensteiner, S. (2013) Chlorophyll breakdown: chemistry, biochemistry and biology. In *Handbook of Porphyrin Science* (Ferreira, G.C., Kadish, K.M., Smith, K.M. and Guilard, R. eds). Hackensack, NJ, USA: World Scientific Publishing, pp. 117-185.

Kräutler, B., Jaun, B., Bortlik, K.-H., Schellenberg, M. and Matile, P. (1991) On the enigma of chlorophyll degradation: the constitution of a secoporphinoid catabolite. *Angew. Chem. Int. Ed. Engl.*, **30**, 1315-1318.

Losey, F.G. and Engel, N. (2001) Isolation and characterization of a urobilinogenoidic chlorophyll catabolite from *Hordeum vulgare* L. *J. Biol. Chem.*, **276**, 27233-27236.

Matile, P., Ginsburg, S., Schellenberg, M. and Thomas, H. (1988) Catabolites of chlorophyll in senescing barley leaves are localized in the vacuoles of mesophyll cells. *Proc. Natl. Acad. Sci. USA*, **85**, 9529-9532.

Moser, S., Müller, T., Ebert, M.O., Jockusch, S., Turro, N.J. and Kräutler, B. (2008a) Blue luminescence of ripening bananas. *Angew. Chem. Int. Ed.*, **47**, 8954-8957.

Moser, S., Müller, T., Holzinger, A., Lutz, C., Jockusch, S., Turro, N.J. and Kräutler, B. (2009) Fluorescent chlorophyll catabolites in bananas light up blue halos of cell death. *Proc. Natl. Acad. Sci. USA*, **106**, 15538-15543.

Moser, S., Ulrich, M., Müller, T. and Kräutler, B. (2008b) A yellow chlorophyll catabolite is a pigment of the fall colours. *Photochem. Photobiol. Sci.*, **7**, 1577-1581.

Mühlecker, W. and Kräutler, B. (1996) Breakdown of chlorophyll: constitution of nonfluorescing chlorophyll-catabolites from senescent cotyledons of the dicot rape. *Plant Physiol. Biochem.*, **34**, 61-75.

Mühlecker, W., Kräutler, B., Moser, D., Matile, P. and Hörtensteiner, S. (2000) Breakdown of chlorophyll: a fluorescent chlorophyll catabolite from sweet pepper (*Capsicum annuum*). *Helv. Chim. Acta*, **83**, 278-286.

Mühlecker, W., Ongania, K.-H., Kräutler, B., Matile, P. and Hörtensteiner, S. (1997) Tracking down chlorophyll breakdown in plants: elucidation of the constitution of a 'fluorescent' chlorophyll catabolite. *Angew. Chem. Int. Ed. Engl.*, **36**, 401-404.

Müller, T., Moser, S., Ongania, K.-H., Pružinská, A., Hörtensteiner, S. and Kräutler, B. (2006) A divergent path of chlorophyll breakdown in the model plant *Arabidopsis thaliana*. *ChemBioChem*, **7**, 40-42.

Müller, T., Ulrich, M., Ongania, K.H. and Kräutler, B. (2007) Colorless tetrapyrrolic chlorophyll catabolites found in ripening fruit are effective antioxidants. *Angew. Chem. Int. Ed.*, **46**, 8699-8702.

Müller, T., Vergeiner, S. and Kräutler, B. (2014) Structure elucidation of chlorophyll catabolites (phyllobilins) by ESI-mass spectrometry - Pseudo-molecular ions and fragmentation analysis of a nonfluorescent chlorophyll catabolite (NCC). *Int. J. Mass Spec.*, **365-366**, 48-55.

Mur, L.A.J., Aubry, S., Mondhe, M., Kingston-Smith, A., Gallagher, J., Timms-Taravella, E., James, C., Papp, I., Hörtensteiner, S., Thomas, H. and Ougham, H. (2010) Accumulation of chlorophyll catabolites photosensitizes the hypersensitive response elicited by *Pseudomonas syringae* in Arabidopsis. *New Phytol.*, **188**, 161-174.

Nakajima, S., Ito, H., Tanaka, R. and Tanaka, A. (2012) Chlorophyll *b* reductase plays an essential role in maturation and storability of Arabidopsis seeds. *Plant Physiology*, **160**, 261-273.

Nordborg, M., Hu, T.T., Ishino, Y., Jhaveri, J., Toomajian, C., Zheng, H.G., Bakker, E., Calabrese, P., Gladstone, J., Goyal, R., Jakobsson, M., Kim, S., Morozov, Y., Padhukasahasram, B., Plagnol, V., Rosenberg, N.A., Shah, C., Wall, J.D., Wang, J., Zhao, K.Y., Kalbfleisch, T., Schulz, V., Kreitman, M. and Bergelson, J. (2005) The pattern of polymorphism in *Arabidopsis thaliana*. *Plos Biol.*, **3**, 1289-1299.

Oberhuber, M., Berghold, J., Breuker, K., Hörtensteiner, S. and Kräutler, B. (2003) Breakdown of chlorophyll: a nonenzymatic reaction accounts for the formation of the colorless "nonfluorescent" chlorophyll catabolites. *Proc. Natl. Acad. Sci. USA*, **100**, 6910-6915.

Oberhuber, M., Berghold, J., Mühlecker, W., Hörtensteiner, S. and Kräutler, B. (2001) Chlorophyll breakdown - on a nonfluorescent chlorophyll catabolite from spinach. *Helv. Chim. Acta*, **84**, 2615-2627.

Pružinská, A., Anders, I., Aubry, S., Schenk, N., Tapernoux-Lüthi, E., Müller, T., Kräutler, B. and Hörtensteiner, S. (2007) In vivo participation of red chlorophyll catabolite reductase in chlorophyll breakdown. *Plant Cell*, **19**, 369-387.

Pružinská, A., Anders, I., Tanner, G., Roca, M. and Hörtensteiner, S. (2003) Chlorophyll breakdown: pheophorbide *a* oxygenase is a Rieske-type iron-sulfur protein, encoded by the *accelerated cell death 1* gene. *Proc. Natl. Acad. Sci. USA*, **100**, 15259-15264.

Pružinská, A., Tanner, G., Aubry, S., Anders, I., Moser, S., Müller, T., Ongania, K.-H., Kräutler, B., Youn, J.-Y., Liljegren, S.J. and Hörtensteiner, S. (2005) Chlorophyll breakdown in senescent

Arabidopsis leaves: characterization of chlorophyll catabolites and of chlorophyll catabolic enzymes involved in the degreening reaction. *Plant Physiol.*, **139**, 52-63.

Rios, J.J., Perez-Galvez, A. and Roca, M. (2014a) Non-fluorescent chlorophyll catabolites in quince fruits. *Food Res. Int.*, **65**, 255-262.

Rios, J.J., Roca, M. and Perez-Galvez, A. (2014b) Nonfluorescent chlorophyll catabolites in loquat fruits (*Eriobotrya japonica* Lindl.). *J. Agric. Food Chem.*, **62**, 10576-10584.

Rios, J.J., Roca, M. and Perez-Galvez, A. (2015) Systematic HPLC/ESI-high resolution-qTOF-MS methodology for metabolomic studies in nonfluorescent chlorophyll catabolites pathway. *J. Anal. Methods Chem.*, **2015**, 490627.

Rodoni, S., Mühlecker, W., Anderl, M., Kräutler, B., Moser, D., Thomas, H., Matile, P. and Hörtensteiner, S. (1997) Chlorophyll breakdown in senescent chloroplasts. Cleavage of pheophorbide *a* in two enzymic steps. *Plant Physiol.*, **115**, 669-676.

Sawada, Y., Nakabayashi, R., Yamada, Y., Suzuki, M., Sato, M., Sakata, A., Akiyama, K., Sakurai, T., Matsuda, F., Aoki, T., Hirai, M.Y. and Saito, K. (2012) RIKEN tandem mass spectral database (ReSpect) for phytochemicals: A plant-specific MS/MS-based data resource and database. *Phytochemistry*, **82**, 38-45.

Smith, C.A., O'Maille, G., Want, E.J., Qin, C., Trauger, S.A., Brandon, T.R., Custodio, D.E., Abagyan, R. and Siuzdak, G. (2005) METLIN - a metabolite mass spectral database. *Ther. Drug Monit.*, **27**, 747-751.

Strain, H.H., Cope, B.T. and Svec, W.A. (1971) Analytical procedures for the isolation, identification, estimation and investigation of the chlorophylls. *Methods Enzymol.*, **23**, 452-476.

Süssenbacher, I., Christ, B., Hörtensteiner, S. and Kräutler, B. (2014) Hydroxymethylated phyllobilins: A puzzling new feature of the dioxobilin branch of chlorophyll breakdown. *Chem.-Eur. J.*, **20**, 87-92.

Süssenbacher, I., Christ, B., Hörtensteiner, S. and Kräutler, B. (2015) Hydroxymethylated phyllobilins in senescent *Arabidopsis thaliana* leaves - sign of a puzzling intermezzo of chlorophyll breakdown. *Chem.-Eur. J.*, **21**, 11664-11670.

Tautenhahn, R., Patti, G.J., Rinehart, D. and Siuzdak, G. (2012) XCMS online: a web-based platform to process untargeted metabolomic data. *Anal. Chem.*, **84**, 5035-5039.

Vergeiner, C., Ulrich, M., Li, C.J., Liu, X.J., Müller, T. and Kräutler, B. (2015) Stereo- and regioselective phyllobilane oxidation in leaf homogenates of the peace lily (*Spathiphyllum wallisii*): hypothetical endogenous path to yellow chlorophyll catabolites. *Chem-Eur J*, **21**, 136-149.

Willstätter, R. and Stoll, A. (1913) Die Wirkungen der Chlorophyllase. In *Untersuchungen über Chlorophyll* (Willstätter, R. and Stoll, A. eds). Berlin: Verlag Julius Springer, pp. 172-187.

Wüthrich, K.L., Bovet, L., Hunziker, P.E., Donnison, I.S. and Hörtensteiner, S. (2000) Molecular cloning, functional expression and characterisation of RCC reductase involved in chlorophyll catabolism. *Plant J.*, **21**, 189-198.

Figure legends

Figure 1

The PAO/phyllobilin pathway of chlorophyll breakdown in Arabidopsis. Chlorophyll is converted to *primary* FCC, which after export from the chloroplast is modified at different sites as shown. These modifications give rise to a variety of fluorescent phyllobilins (DFCCs and FCCs) that after import into the vacuole are isomerized to respective DNCCs and NCCs. R^1-R^3 indicate phyllobilin modifications according to Table 1. In *primary* FCC, pyrrole rings (A-D) and relevant atoms are labeled. The types of modifications and the known enzymes catalyzing them are shown. Question marks indicate that enzymes responsible for respective modifications are unknown. DFCC, dioxobilin-type fluorescent chlorophyll catabolite; DNCC, dioxobilin-type nonfluorescent chlorophyll catabolite; ER, endoplasmic reticulum; FCC, formyloxobilin-type fluorescent chlorophyll catabolite; NCC, formyloxobilin-type nonfluorescent chlorophyll catabolite.

Figure 2

Fast LC separation and MS(/MS) identification of phyllobilins from Arabidopsis wild-type (Col-0). (a) Base peak chromatogram (BPC) of a green leaf extract. (b-d) Analysis of catabolites from senescent Col-0 leaves, comparing UV absorption at 254 nm (b), BPC (c) and extracted ion chromatograms (EICs) of all detected phyllobilins (d). Note that phyllobilins specifically accumulate in senescent leaf samples. For MS and MS/MS spectral details of the phyllobilins, see Table 1, Table S1 and Figure S1. Only the major phyllobilin isomers (see Figure S2) are labeled.

Figure 3

MS and MS/MS spectra of Arabidopsis Col-0 phyllobilins. Selected MS (top) and MS/MS (bottom) spectra of a known (a, DNCC_618) and a novel (b, DNCC_780) phyllobilin are shown. For the MS and MS/MS spectra of all 16 phyllobilins identified in this work, see Figure S1. Constitutional formulae and MS/MS fragmentation sites are shown. P^+, protonated precursor ion.

Figure 4

Base peak (BPCs) and extracted ion chromatograms (EICs) of senescent leaf extracts from Arabidopsis chlorophyll catabolic mutants. For MS and MS/MS spectral details of the identified phyllobilins, see Table 1, Table S1 and Figure S1. In each chromatogram, only the major phyllobilin isomers (see Figure S2) are labeled.

Figure 5

Phyllobilin quantification. (a) A principle component analysis illustrates that metabolic profiles of senescent leaves of wild-type (Col-0) and different chlorophyll catabolic mutants are distinct. (b-d) Comparison of UV/Vis- and MS ionization-based quantification of phyllobilins in Col-0 and single chlorophyll catabolic mutants. Data are mean+SD of four biological replicates.

Figure 6

LC-MS analysis of phyllobilins in different Arabidopsis ecotypes and other plant species. (a-d) The Arabidopsis phyllobilin MS library created with the data of this work was used to quantify phyllobilin modifications across 18 Arabidopsis ecotypes. Data are mean+SD of four biological replicates. (e) Identification of Arabidopsis-like phyllobilins in other plant species. Extracted ion chromatograms (EICs) of phyllobilins identified in respective tissues are shown. Note that several phyllobilins detected in canola and spinach have not been described before in these species. Note also that spinach and pear possess type-2 RCCRs, hence produce C16 isomers of the respective phyllobilins in Arabidopsis or canola. This explains the shifted retention times of the spinach and pear phyllobilins as compared to canola and Arabidopsis (see also Figures 2 and 4).

Table 1. Arabidopsis phyllobilins identified in this work.

Assigned Name	Presence[1]	Library ID[2]	m/z [M+H]$^+$ measured	m/z [M+H]$^+$ calculated	Formula (M)	Side chain modifications[3]			Retention time[4]	Other names	MS/MS[5]	NMR data[6]	Reference
						R^1 ($C3^2$)	R^2 ($O8^4$)	R^3 (C2/C4)					
DNCC_602	co	3^{co}	603.2817	603.2813	$C_{33}H_{38}N_4O_7$	H	H	H	5.3	*At*-DNCC-45, *At*-DNCC-48	34.4	+	Süssenbacher *et al*. 2015
DNCC_616	me	9^{me}	617.2966	617.2970	$C_{34}H_{40}N_4O_7$	H	CH_3	H	6.0	*At-mes16*-DNCC-47	35.0	+	Süssenbacher *et al*. 2014
DNCC_618	co	1^{co}	619.2756	619.2762	$C_{33}H_{38}N_4O_8$	OH	H	H	3.1	*At*-DNCC-1, *At*-DNCC-33	35.1	+	Christ *et al*. 2013; Süssenbacher *et al*. 2015
DNCC_632-1	co	2^{co}	633.2910	633.2919	$C_{34}H_{40}N_4O_8$	H	H	C4-HM	4.4	*At*-4HM-DNCC-41	35.5	+	Süssenbacher *et al*. 2015
DNCC_632-2	co	15^{co}	633.2907	633.2919	$C_{34}H_{40}N_4O_8$	H	H	C2-HM	4.6	*At*-2HM-*iso*-DNCC-42	35.5	+	Süssenbacher *et al*. 2015
DNCC_632-3	me	7^{me}	633.2913	633.2919	$C_{34}H_{40}N_4O_8$	OH	CH_3	H	4.2	*At-mes16*-DNCC-38	35.5	+	Süssenbacher *et al*. 2014
DNCC_646-1	me	8^{me}	647.3071	647.3075	$C_{35}H_{42}N_4O_8$	H	CH_3	C4-HM	5.2	*At-mes16*-9HM-DNCC-44	35.9	+	Süssenbacher *et al*. 2014
DNCC_646-2	me	16^{me}	647.3068	647.3075	$C_{35}H_{42}N_4O_8$	H	CH_3	C2-HM	5.4	*At-mes16*-7HM-*iso*-DNCC-46	35.9	+	Süssenbacher *et al*. 2014
DNCC_780	co	13^{co}	781.3293	781.3291	$C_{39}H_{48}N_4O_{13}$	OGlc	H	H	2.1	-	39.4	-	This work
DNCC_794	me	14^{me}	795.3459	795.3447	$C_{40}H_{50}N_4O_{13}$	OGlc	CH_3	H	2.9	-	39.7	-	This work
NCC_614	co,cy	5^{cy}	615.2808	615.2813	$C_{34}H_{38}N_4O_7$	H	H	H	6.4	*At*-NCC-5	35.0	+	Pruzinska *et al*. 2005
NCC_628	me,cm	12^{cm}	629.2981	629.2970	$C_{35}H_{40}N_4O_7$	H	CH_3	H	7.6	*mes16*-FCC-3[8]	35.4	+	Christ *et al*. 2012
NCC_630	co,cy	4^{cy}	631.2753	631.2762	$C_{34}H_{38}N_4O_8$	OH[7]	H	H	4.5	*At*-NCC-2/*At*-NCC-3[7]	35.4	+	Pružinská *et al*. 2005
NCC_644	me,cy,cm	11^{cm}	645.2913	645.2919	$C_{35}H_{40}N_4O_8$	OH	CH_3	H	5.3	*mes16*-FCC-2[8]	35.8	+	Christ *et al*. 2012
NCC_792	co,cy	6^{cy}	793.3281	793.3291	$C_{40}H_{48}N_4O_{13}$	OGlc	H	H	2.6	*At*-NCC-1	39.7	+	Pružinská *et al*. 2005
NCC_806	co,me,cy,cm	10^{cm}	807.3451	807.3447	$C_{41}H_{50}N_4O_{13}$	OGlc	CH_3	H	3.5	*At*-NCC-4	40.0	+	Pružinská *et al*. 2005

[1]co, Col-0; me, *mes16-1*; cy, *cyp89a9-1*; cm, *cyp89a9-1*/*mes16-1*; [2]for source of spectra used in the Arabidopsis phyllobilin MS library, see footnote[1]; [3]positions of modifications as depicted in Figure 1; HM, hydroxymethyl; Glc, glucosyl; [4]only retention time [min] of the major isomer of each phyllobilin is shown; see EICs of Figure S2, for the retention times of all isomers; [5]+, pyllobilins for which NMR data have been published; [7]collision energies [eV] used for the MS/MS fragmentation experiments shown in Figures 3 and S1 and in Table S1; [7]the major isomer likely corresponds to *At*-NCC-2, with OH being located at $C8^2$ (see Figure S2, for respective EICs); [8]to date, these catabolites have only been identified as their respective fluorescent isomers.

Figure 1

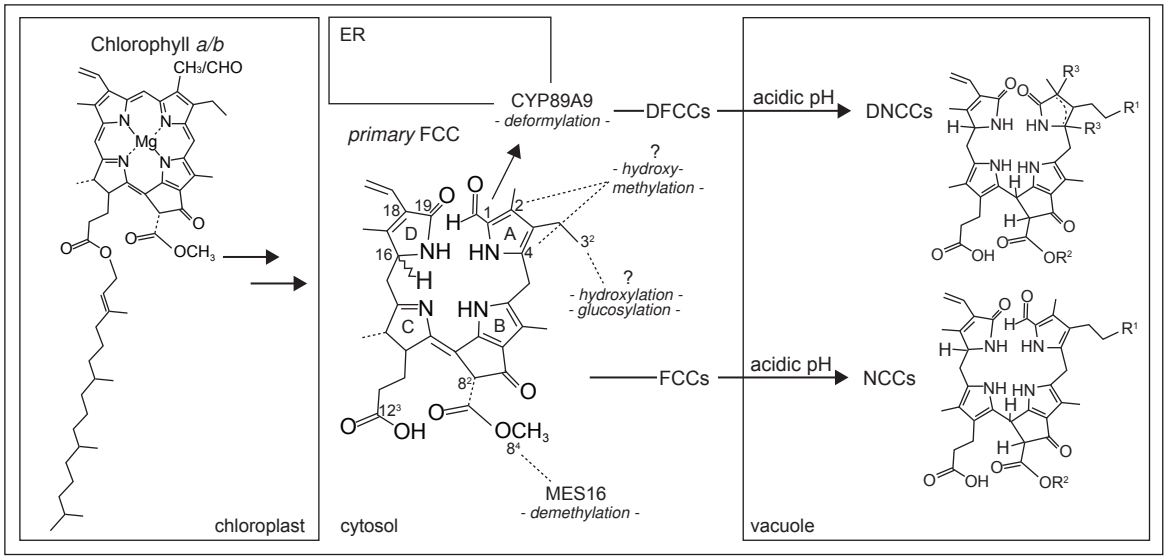

Figure 1. The PAO/phyllobilin pathway of chlorophyll breakdown in Arabidopsis. Chlorophyll is converted to *primary* FCC, which after export from the chloroplast is modified at different sites as shown. These modifications give rise to a variety of fluorescent phyllobilins (DFCCs and FCCs) that after import into the vacuole are isomerized to respective DNCCs and NCCs. R^1-R^3 indicate phyllobilin modifications according to Table 1. In *primary* FCC, pyrrole rings (A-D) and relevant atoms are labeled. The types of modifications and the known enzymes catalyzing them are shown. Question marks indicate that enzymes responsible for respective modifications are unknown. DFCC, dioxobilin-type fluorescent chlorophyll catabolite; DNCC, dioxobilin-type nonfluorescent chlorophyll catabolite; ER, endoplasmic reticulum; FCC, formyloxobilin-type fluorescent chlorophyll catabolite; NCC, formyloxobilin-type nonfluorescent chlorophyll catabolite.

Figure 2

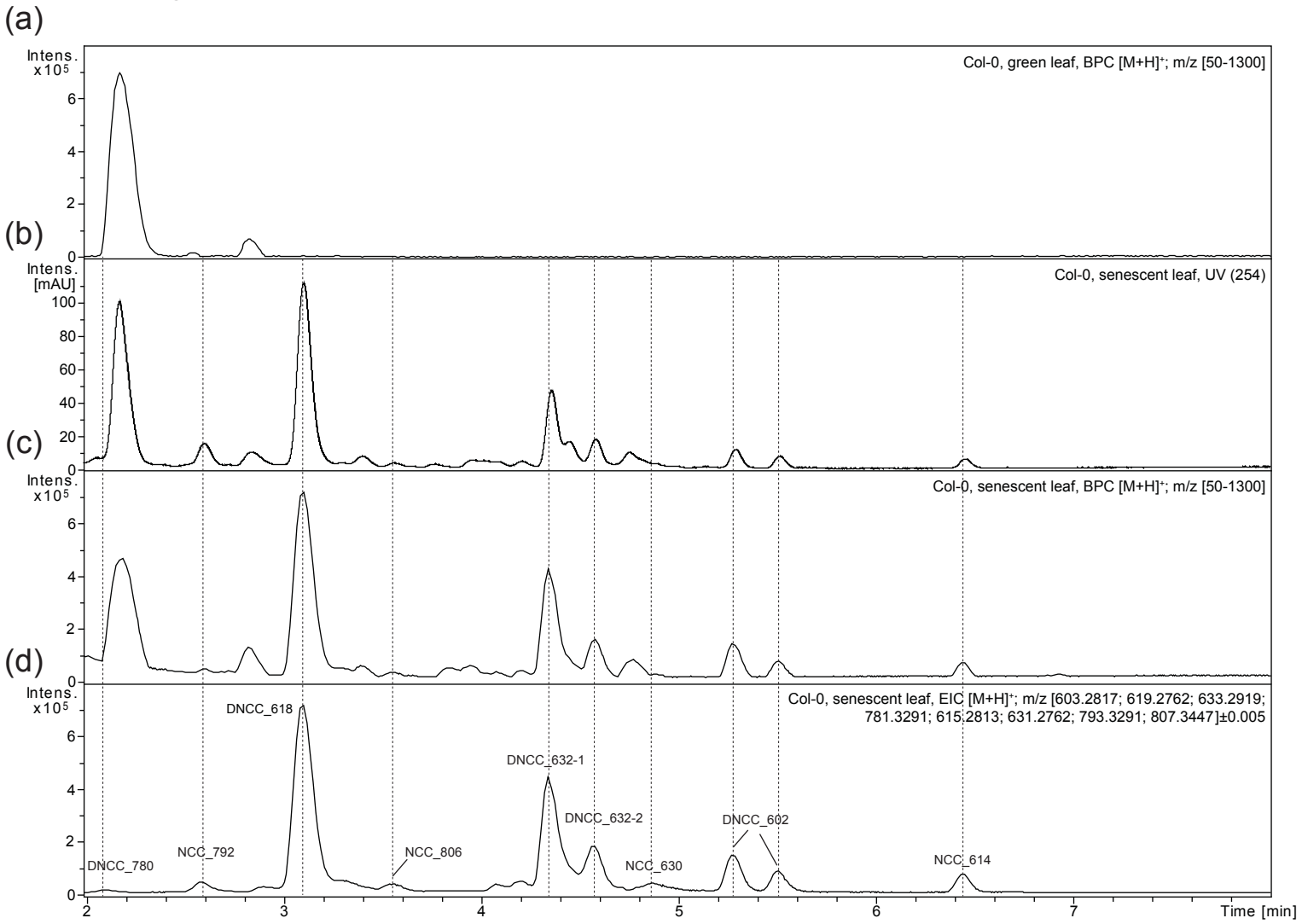

Figure 2. Fast LC separation and MS(/MS) identification of phyllobilins from Arabidopsis wild-type (Col-0). (a) Base peak chromatogram (BPC) of a green leaf extract. (b-d) Analysis of catabolites from senescent Col-0 leaves, comparing UV absorption at 254 nm (b), BPC (c) and extracted ion chromatograms (EICs) of all detected phyllobilins (d). Note that phyllobilins specifically accumulate in senescent leaf samples. For MS and MS/MS spectral details of the phyllobilins, see Table 1, Table S1 and Figure S1. Only the major phyllobilin isomers (see Figure S2) are labeled.

Figure 3

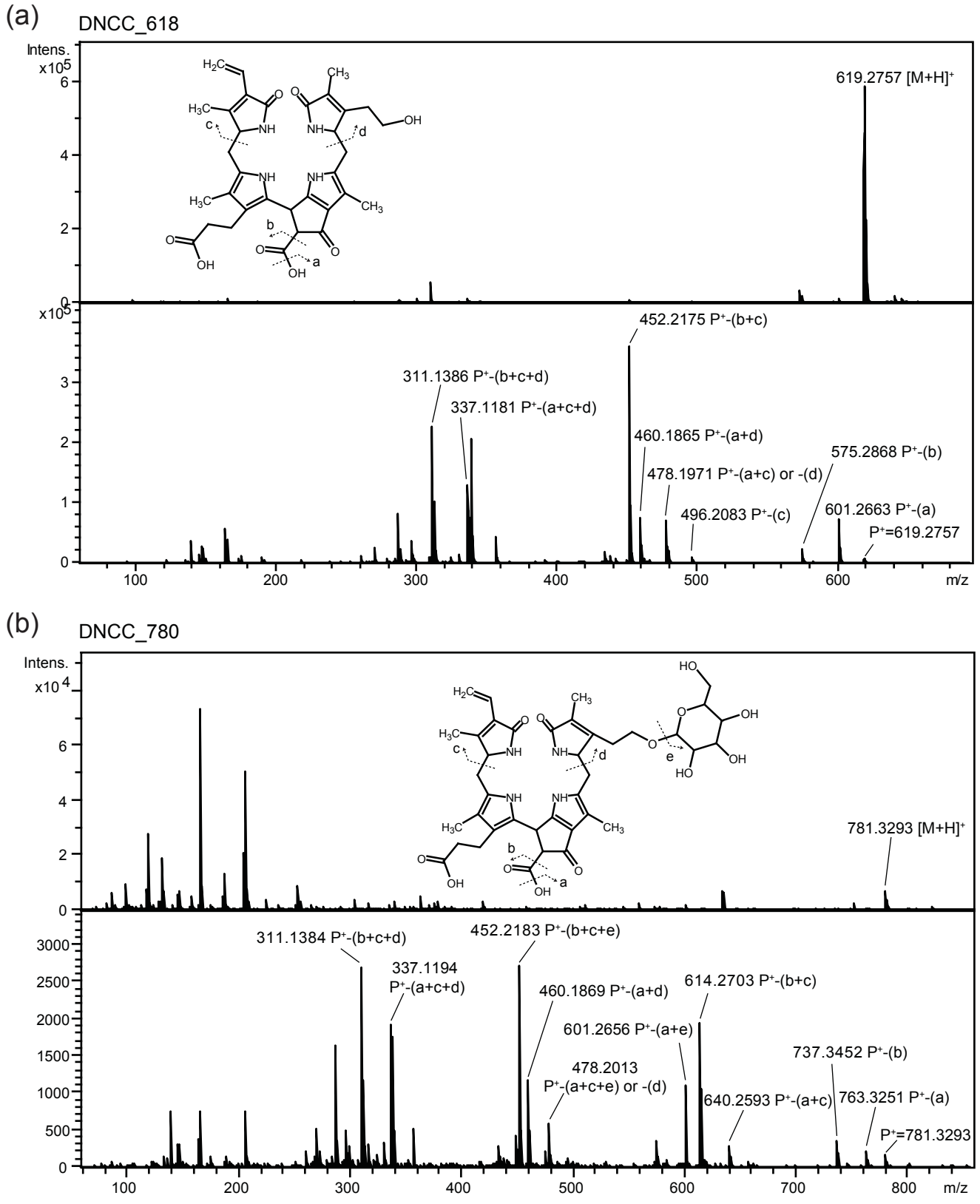

Figure 3. MS and MS/MS spectra of Arabidopsis Col-0 phyllobilins. Selected MS (top) and MS/MS (bottom) spectra of a known (a, DNCC_618) and a novel (b, DNCC_780) phyllobilin are shown. For the MS and MS/MS spectra of all 16 phyllobilins identified in this work, see Figure S1. Constitutional formulae and MS/MS fragmentation sites are shown. P+, protonated precursor ion.

Figure 4

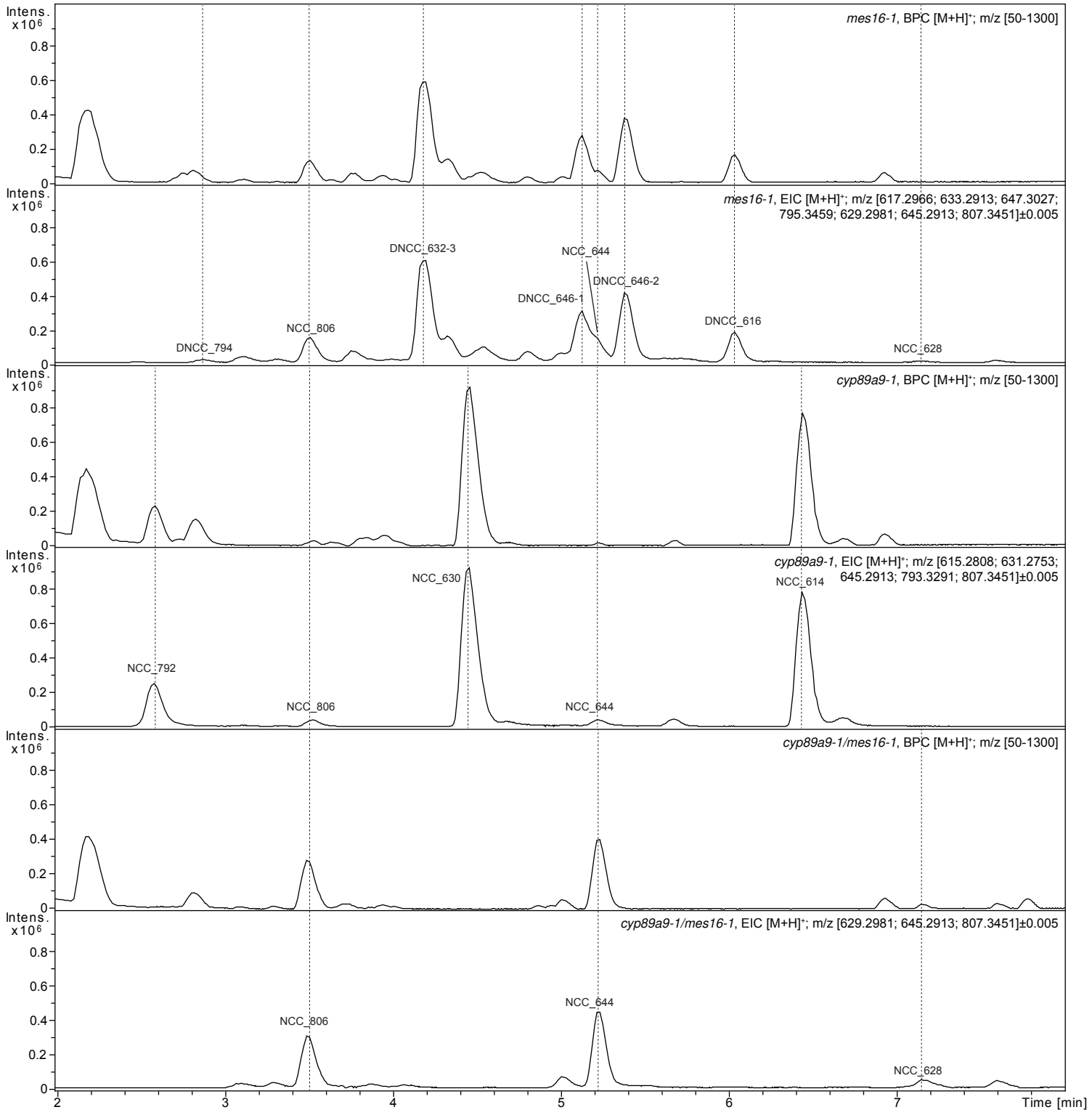

Figure 4. Base peak (BPCs) and extracted ion chromatograms (EICs) of senescent leaf extracts from Arabidopsis chlorophyll catabolic mutants. For MS and MS/MS spectral details of the identified phyllobilins, see Table 1, Table S1 and Figure S1. In each chromatogram, only the major phyllobilin isomers (see Figure S2) are labeled.

Figure 5

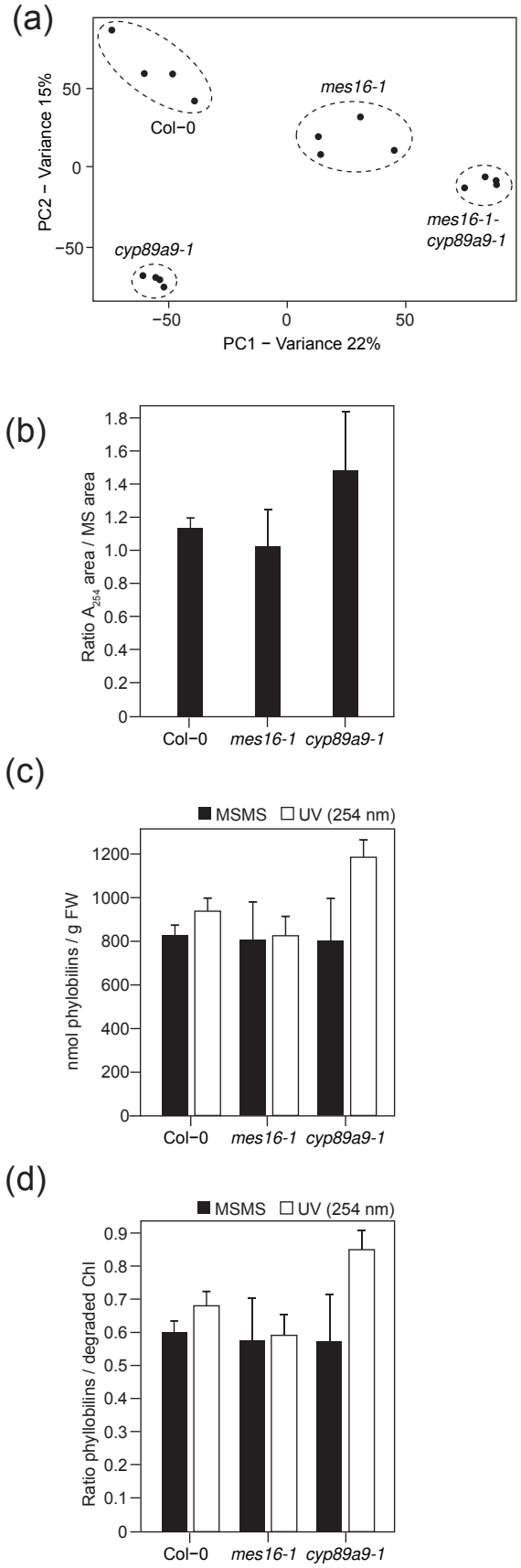

Figure 5. Phyllobilin quantification. (a) A principle component analysis illustrates that metabolic profiles of senescent leaves of wild-type (Col-0) and different chlorophyll catabolic mutants are distinct. (b-d) Comparison of UV/Vis- and MS ionization-based quantification of phyllobilins in Col-0 and single chlorophyll catabolic mutants. Data are mean+SD of four biological replicates.

Figure 6

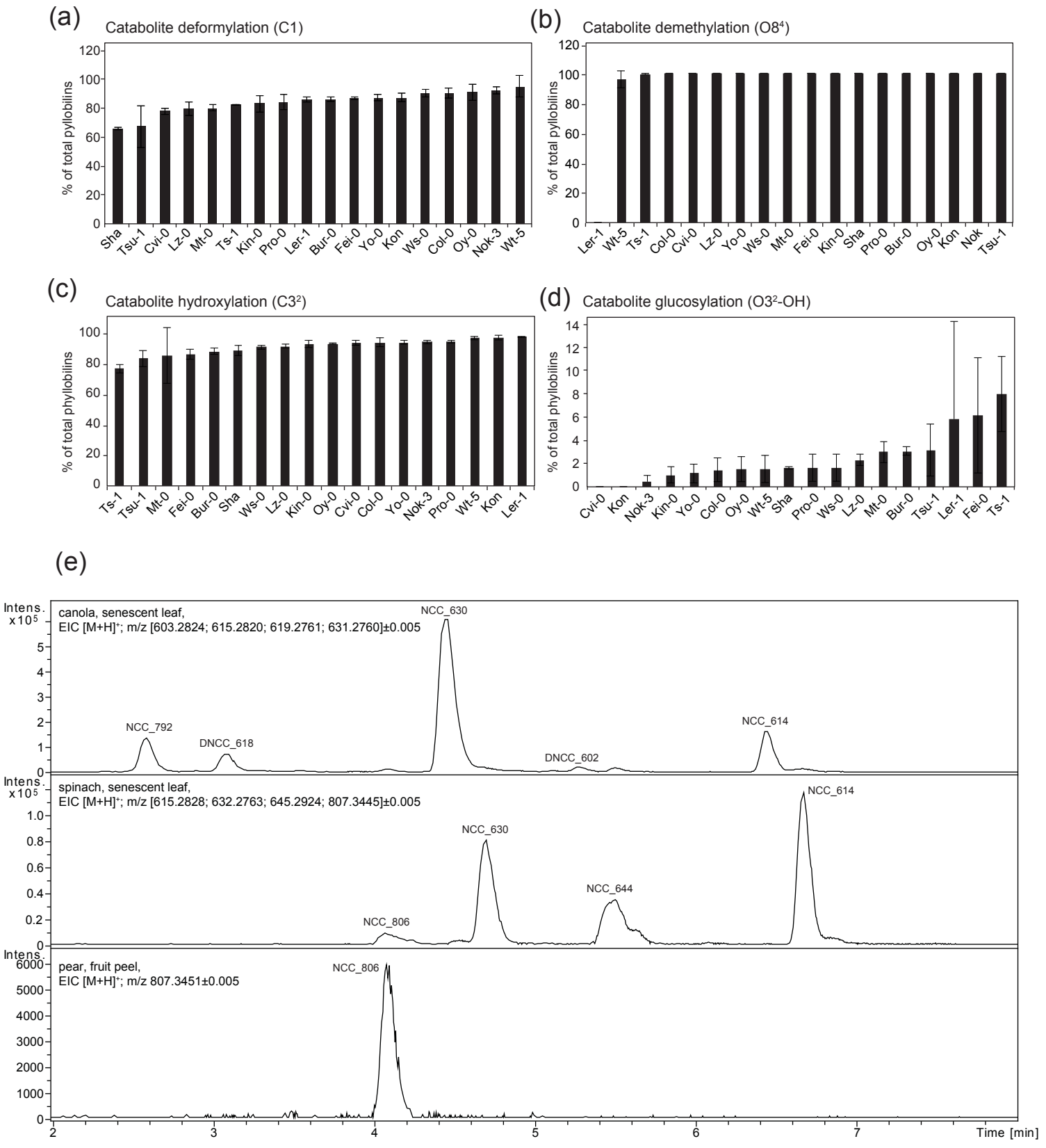

Figure 6. LC-MS analysis of phyllobilins in different Arabidopsis ecotypes and other plant species. (a-d) The Arabidopsis phyllobilin MS library created with the data of this work was used to quantify phyllobilin modifications across 18 Arabidopsis ecotypes. Data are mean+SD of four biological replicates. (e) Identification of Arabidopsis-like phyllobilins in other plant species. Extracted ion chromatograms (EICs) of phyllobilins identified in respective tissues are shown. Note that several phyllobilins detected in canola and spinach have not been described before in these species. Note also that spinach and pear possess type-2 RCCRs, hence produce C16 isomers of the respective phyllobilins in Arabidopsis or canola. This explains the shifted retention times of the spinach and pear phyllobilins as compared to canola and Arabidopsis (see also Figures 2 and 4).